ACS central science

Research Article

http://pubs.acs.org/journal/acscii

High-Throughput Excipient Discovery Enables Oral Delivery of Poorly Soluble Pharmaceuticals

Jeffrey M. Ting,[†,‡] Swapnil Tale,[§] Anatolii A. Purchel,[§] Seamus D. Jones,[†] Lakmini Widanapathirana,[§] Zachary P. Tolstyka,[§] Li Guo,[∥] Steven J. Guillaudeu,[∥] Frank S. Bates,[*,†] and Theresa M. Reineke[*,§]

[§]Department of Chemistry and [†]Department of Chemical Engineering and Materials Science, University of Minnesota, Minneapolis, Minnesota 55455, United States

[∥]Corporate R&D, The Dow Chemical Company, Midland, Michigan 48674, United States

Supporting Information

ABSTRACT: Polymeric excipients are crucial ingredients in modern pills, increasing the therapeutic bioavailability, safety, stability, and accessibility of lifesaving products to combat diseases in developed and developing countries worldwide. Because many early-pipeline drugs are clinically intractable due to hydrophobicity and crystallinity, new solubilizing excipients can reposition successful and even failed compounds to more effective and inexpensive oral formulations. With assistance from high-throughput controlled polymerization and screening tools, we employed a strategic, molecular evolution approach to systematically modulate designer excipients based on the cyclic imide chemical groups of an important (yet relatively insoluble) drug phenytoin. In these acrylamide- and methacrylate-containing polymers, a synthon approach was employed: one monomer served as a precipitation inhibitor for phenytoin recrystallization, while the comonomer provided hydrophilicity. Systems that maintained drug supersaturation in amorphous solid dispersions were identified with molecular-level understanding of noncovalent interactions using NOESY and DOSY NMR spectroscopy. Poly(*N*-isopropylacrylamide-*co*-*N*,*N*-dimethylacrylamide) (poly(NIPAm-*co*-DMA)) at 70 mol % NIPAm exhibited the highest drug solubilization, in which phenytoin associated with inhibiting NIPAm units only with lowered diffusivity in solution. In vitro dissolution tests of select spray-dried dispersions corroborated the screening trends between polymer chemical composition and solubilization performance, where the best NIPAm/DMA polymer elevated the mean area-under-the-dissolution-curve by 21 times its crystalline state at 10 wt % drug loading. When administered to rats for pharmacokinetic evaluation, the same leading poly(NIPAm-*co*-DMA) formulation tripled the oral bioavailability compared to a leading commercial excipient, HPMCAS, and translated to a remarkable 23-fold improvement over crystalline phenytoin.

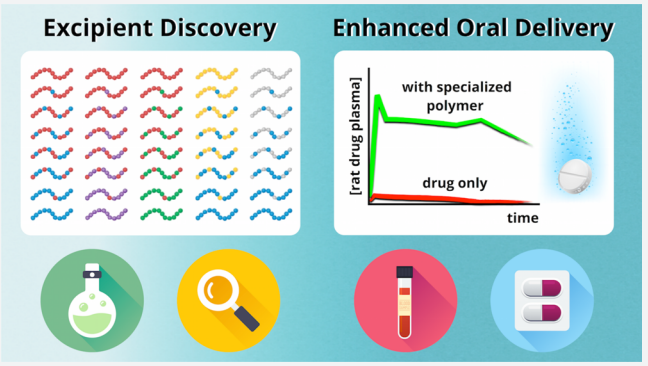

Oral drug administration is the most widespread, cost-effective, and appealing drug delivery strategy to treat afflictions and advance human health and well-being worldwide. In the past decade, breakthrough oral medicines have been under development to address common infectious diseases and chronic ailments such as diabetes mellitus,[1] hypertension,[2] and HIV.[3] Successful commercialization of such noninvasive medications to global markets has driven tremendous interest to explore new carrier compounds and molecular targets through oral delivery, even igniting ambitious efforts to transport biopharmaceuticals (nucleic acids, antibodies, proteins)[4] across physiological obstacles like the gastrointestinal tract and blood–brain barrier. Toward these goals, the pharmaceutical field has integrated high-throughput screening (HTS) approaches to increase the prolific pace of early-stage drug discovery by orders of magnitude.[5] However, poor R&D productivity[6] plagues the drug pipeline: on average, developmental times currently span over a decade with less than 12% of clinical trial candidates resulting in approved formulations.[7]

This striking discrepancy results from high drug hydrophobicity and crystallization, which reduce the aqueous solubility required for oral bioavailability[8] and explain the failure of compounds to meet industry guidelines such as Lipinski's rule of five.[9] To mitigate this problem, excipients, inert pharmaceutical ingredients in therapeutic or diagnostic formulations, are employed. These important and commonly polymeric enhancers can encapsulate drugs, stabilize drug potency, prolong shelf life, safeguard against toxicity, or govern programmable release. While many recent attempts have been made to creatively exploit the versatility of polymer science in directing drug delivery efforts,[10−13] there remain enormous opportunities to streamline excipient discovery efforts to complement the HTS of drug candidates (Figure 1A). Currently, there is no overarching U.S. FDA regulatory approval system for new pharmaceutical excipients. In general,

Received: September 7, 2016
Published: October 12, 2016

DOI: 10.1021/acscentsci.6b00268
ACS Cent. Sci. 2016, 2, 748−755

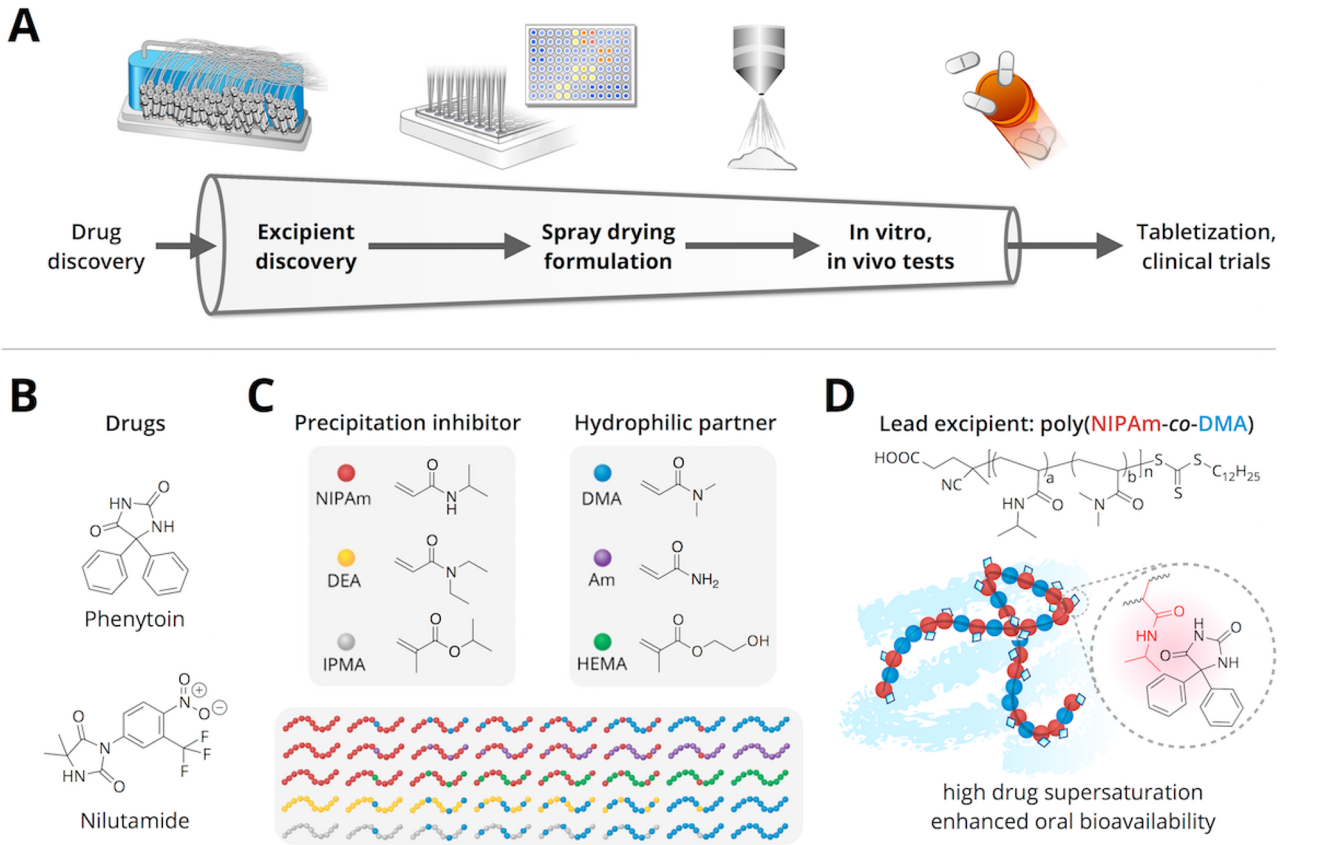

Figure 1. Design of polymer carriers to tailor solubilization for highly hydrophobic drugs of interest. (A) In the excipient development pipeline, high-throughput controlled polymer synthesis and screening tools can expedite the identification and production of specialized oral drug formulations. In this scheme, (B) the cyclic imide groups of phenytoin and nilutamide motivated the (C) synthon approach to construct excipients combinatorially with precipitation inhibitor and hydrophilic units. (D) For spray-dried dispersions with the leading excipient, the NIPAm inhibitor units adsorbed onto amorphized phenytoin to increase the apparent drug solubility by over an order of magnitude.

the introduction of a new excipient is included in standard clinical reports filed during the new drug applications process on an individual basis.[14] Excipients can be designed to form solid dispersions, which advantageously stabilize amorphous drug molecules with noncovalent interactions to circumvent solubility limitations by suppressing crystallization leading to drug supersaturation.[15]

To this end, we have explored various synthetic polymer platforms in a quest to create versatile excipients, tuning molecular architectures, distributions of chemical functionalities, and macromolecular self-assembly to elucidate structure−property relationships between polymers and drugs in robust spray-dried dispersions.[16−19] In our studies, subtle molecular attributes that influence supersaturation such as amphiphilicity, ionic character, and related chemical properties have been identified. However, these functionalities are unable to maintain high supersaturation of drugs with fast recrystallization kinetics. One example is phenytoin (Figure 1B), a highly prescribed and important antiseizure medication on the World Health Organization's (WHO's) List of Essential Medicines.[20] In aqueous settings, phenytoin exhibits low solubility (~0.03 mg/mL), driven by uniaxial crystallization facilitated by −NH to −C═O hydrogen bonding between cyclic imide moieties.[21] We aimed to emulate these motifs by constructing copolymer "synthons" (macromolecules containing structural subunits related to conceivable intermolecular interactions, akin to the deconstruction process taught in retrosynthetic analysis in organic chemistry). These polymer systems provided (i) a precipitation inhibitor that complexes with amorphized free drug through complementary hydrogen bonding and (ii) a compatible hydrophilic partner to promote supersaturation generation (Figure 1C).

Herein, we report the first example of this synthon method to design customized excipients, where controlled polymerization enables the installation of specific chemical handles into well-defined microstructures to disrupt drug recrystallization. To test this framework for phenytoin in a high-throughput manner, we selected *N*-isopropylacrylamide (NIPAm) as the inhibiting monomer due to its secondary amide (Figure 1D) promoting interactions with the selected drug candidate. This monomer was balanced through pairings with hydrophilic comonomers *N*,*N*-dimethylacrylamide (DMA), acrylamide (Am), and 2-hydroxyethyl methacrylate (HEMA) that serve to bridge polymer interactions with aqueous media. We also interchanged the NIPAm secondary amide with a hydrophobic tertiary amide and carboxylate ester in *N*,*N*-diethylacrylamide (DEA) and isopropyl methacrylate (IPMA), respectively. Thus, we rapidly prepared polymer synthon constructs with uniform chain lengths spanning the chemical compositional state-space in a molecular evolution inspired approach, followed by HTS with drugs to identify leading candidates for in vitro and in vivo testing.

The polymer synthon hypothesis was further extended to other heterocyclic aromatic drugs. We screened our excipient libraries with (i) nilutamide (Figure 1B), a potent antiandrogen drug for treating metastatic prostate cancer with the capability

DOI: 10.1021/acscentsci.6b00268
ACS Cent. Sci. 2016, 2, 748−755

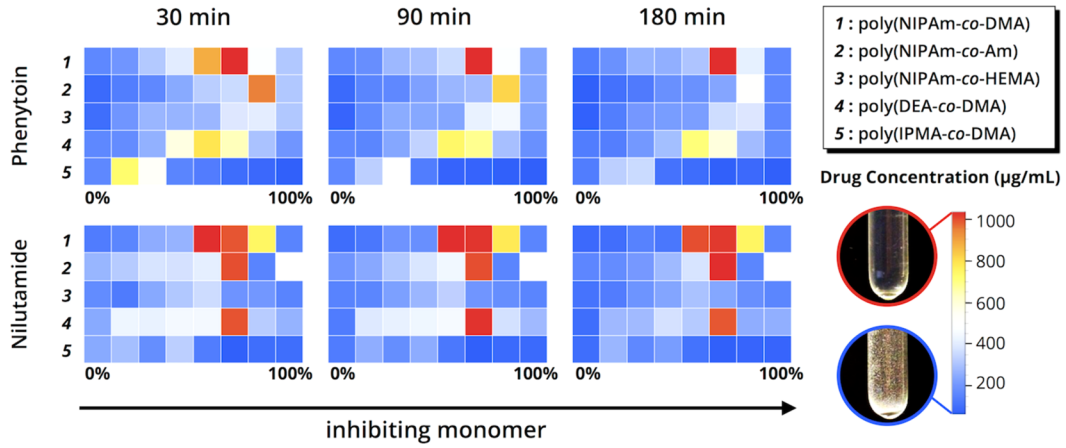

Figure 2. High-throughput precipitation inhibition screening across polymer chemical compositions. Heat map array plots represent supersaturated drug concentrations (average of $N = 3$) of phenytoin and nilutamide over 180 min in PBS solution at 37 °C with polymer synthons 1−5. Across each row in the arrays, the composition of the inhibiting monomer is increasing from 0 to 100 mol %. Experiments were prepared with a total drug concentration of 1000 μg/mL. Details are provided in the Supporting Information.

of crossing the blood−brain barrier,[22] and (ii) griseofulvin, an antifungal drug on the WHO's List of Essential Medicines[20] with latent anticancer activity.[23] These drugs parallel the limited solubility of phenytoin (at 0.004 and 0.05 mg/mL, respectively), but nilutamide contains a similar imide group for −NH to −C═O hydrogen bonding interactions whereas griseofulvin does not. In this manner, the modularity of one set of polymer synthons enables other classes of drugs to be better solubilized into more efficient formulations, such as reducing the necessary therapeutic dosage and developmental cost.

HTS advancements have accelerated the preparation of druglike molecules.[24,25] Comparatively, examples of creating larger, well-defined systems using high-throughput machinery are emerging, such as unimolecular macromolecules[26] and reversible addition−fragmentation chain transfer (RAFT) polymers.[27] We conducted RAFT chemistry on a lab scale first (Figure S-1). The predicted microstructure sequence of monomers was assessed using intrinsic relative reactivities (Figure S-2): all systems except for poly(IPMA-*co*-DMA) (which tends to form blocky sequences) were expected to be statistical or alternating, affording a distribution of inhibiting units along chains.[28] The use of a semicontinuous parallel pressure reactor (Freeslate, Sunnyvale, CA) automated this procedure to rapidly scan chemical compositions at targeted molecular weights. Bulk ingredients (e.g., initiator, monomer, chain transfer agent, solvent) were compartmentalized, dispensed into sealed reactors, and degassed under mechanical stirring. We generated over 60 well-defined RAFT-mediated polymers at targeted molecular weights of 20 and 60 kg/mol with three 8 h experimental runs in parallel. The synthesis procedures and a suite of materials characterization are provided in the Supporting Information.

For supersaturating oral formulations, nonsink dissolution conditions are more appropriate than compendial protocols such as the United States Pharmacopeia (USP), which mandates a 3-fold excess of dissolution media over the volume needed to establish a saturated drug solution. The Sink Index (SI) dimensionless number[29] standardizes the extent of non-USP conditions:

$$\text{sink index} = \frac{C_S}{\text{Dose}/V} < 0.1 \text{ for nonsink setting} \quad (1)$$

Here, C_S is the crystalline drug solubility, Dose is the total drug quantity, and V is the solution volume. Conventional USP apparatuses under sink conditions have a SI > 3. For this work, we targeted a total drug concentration of 1000 μg/mL in both screening and in vitro experiments, corresponding to a calculated SI of 0.09.

To assess drug solubilization enhancement, a precipitation inhibition assay was employed using an automated liquid handler (Freedom EVO 200, Tecan). Drug in methanol was introduced (2% v/v) to a 96-well plate of predissolved polymer in 0.912 mL of phosphate buffered saline (PBS) solution at 37 °C. Although this solvent-shift approach does not fully capture the recrystallization process from solid dispersions, this automated protocol provides rapid assessment of polymer capability to maintain supersaturation. For each experimental assay, the drug supernatant concentration of all prepared polymers was monitored in triplicate. Across the chemical composition spectra of our systems, we observed distinctly promising but narrow leads that were sensitive to monomer constituent combinations (Figure 2). In particular, the sharp transition in the compositional window of poly(NIPAm-*co*-DMA), poly(NIPAm-*co*-Am), and poly(DEA-*co*-DMA) underscores the importance of monomer selection and relative chemical incorporation to facilitate drug supersaturation. For phenytoin and nilutamide, the delicate balance between the inhibitory and hydrophilic monomer is most pronounced around 60−70 mol % inhibiting monomer. For griseofulvin, systems containing these hits succumbed to precipitation over time, irrespective of polymer molecular weight (Figure S-16), and were not studied further.

The leading excipient poly(NIPAm70-*co*-DMA30) (where numbers denote preceding monomer molar compositions) maintained phenytoin supersaturation at 1000 μg/mL over 180 min. This compositional trend was invariant to polymer molecular weight (Figure S-16). To the extent of our knowledge, no other reported solid dispersion excipient has successfully suppressed phenytoin crystallization at this SI. For instance, a leading commercial excipient, hydroxypropyl methyl cellulose acetate succinate (HPMCAS), was reported to maintain phenytoin at 100 μg/mL (SI = 0.9) for 180 min, a poor performance relative to the success of other hydrophobic drugs with HPMCAS in the same study.[13] As seen in Figure 2,

DOI: 10.1021/acscentsci.6b00268
ACS Cent. Sci. 2016, 2, 748−755

other optimal polymer synthons that facilitated high initial phenytoin concentrations (such as poly(NIPAm73-*co*-Am27) or poly(DEA65-*co*-DMA35)) precipitated over time. In comparison, the leading excipients maintained high nilutamide concentrations at similar compositional windows. Collectively, these results suggest that analogous excipient interactions may stabilize supersaturated nilutamide, and alternative tunable synthons need to be built around griseofulvin.

To better examine the discrete interactions of phenytoin with the lead compositions among all polymer systems, we employed 2D nuclear Overhauser effect spectroscopy (NOESY) NMR in deuterated PBS. NOESY experiments rely on transient nuclear Overhauser effect (NOE) enhancements and provide conformational analysis of molecules in solution. In the poly(NIPAm70-*co*-DMA30) spectrum, strong NOE cross correlations were observed between the aromatic proton peaks of phenytoin and the NIPAm isopropyl proton signals (Figure 3 A), indicating that phenytoin molecules were in close spatial proximity to NIPAm monomers only. Although NOESY cannot unequivocally identify modes of hydrogen bonding in deuterated water, a comparison across all leading compositions for each system (Figures S-18–S-22) shows that DMA participates as a compatible hydrophilic monomer for NIPAm in leveraging intermolecular interactions toward amorphized drug molecules. Moreover, the choice of the hydrophilic partner copolymerized with the precipitation inhibitory monomer is important. For example, in the NOESY spectrum of poly(NIPAm73-*co*-Am27) and phenytoin, no cross peaks were observed between the drug phenyl protons and monomer constituents (Figure S-19), despite the presence of a similar NIPAm composition. We speculated that because the hydrophilic monomer (Am) can both donate and accept strong hydrogen bonding interactions, intramolecular polymer interactions precluded polymer/phenytoin complexation. This result was in agreement with the high-throughput precipitation inhibition screening, in which the poly(NIPAm73-*co*-Am27) system exhibited rapid desupersaturation over time.

In principle, strong polymer–drug intermolecular interactions should accompany a decrease in drug diffusivity, which can be quantified with diffusion ordered spectroscopy (DOSY) NMR.[30] We monitored the translational diffusion coefficient (D_0) of saturated phenytoin with increasing polymer concentration (0 to 1000 μg/mL). In all experiments, the diffusion coefficient of a trimethylsilyl propanoic acid (TMSP) standard additive was also measured across all systems to verify that polymer viscosity did not contribute to decreased diffusivity. For the poly(NIPAm70-*co*-DMA30) system, the phenytoin D_0 gradually decreased from $(4.46 \pm 0.02) \times 10^{-10}$ to $(3.72 \pm 0.19) \times 10^{-10}$ m^2/s as polymer concentration increased, and the binding strength (K_b) was calculated to be 44 ± 12 L/mol, which was close in predictive agreement with experimental measurements (Figure 3B). This value was also greater than twice the K_b of all other lead systems (Figure S-24). Together, the NOESY and DOSY NMR experiments provide molecular level understanding of how poly(NIPAm70-*co*-DMA30) facilitates high levels of phenytoin supersaturation maintenance in solution. Similar NMR studies of nilutamide and griseofulvin are the subjects of future investigations. For solid dispersions, this represents a unique way to probe solution-state interactions and construct design principles between polymers and active molecules before scale-up formulation efforts.

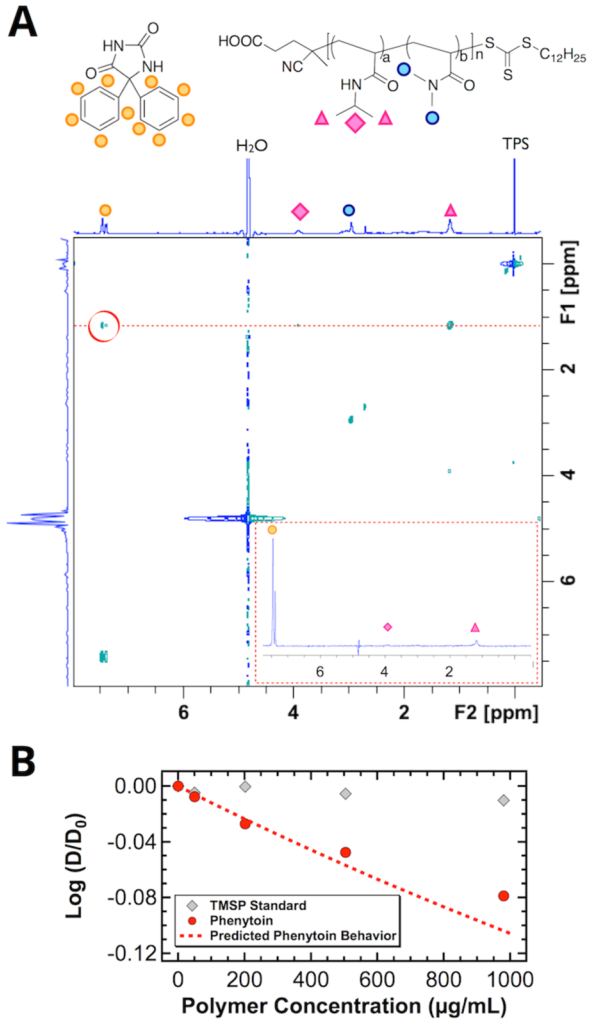

Figure 3. Representative 2D NMR experiments for poly(NIPAm70-*co*-DMA30) in deuterated PBS solution. (A) NOESY NMR spectroscopy shows that aromatic protons of phenytoin (600 μg/mL) were in close spatial proximity to the NIPAm isopropyl protons of the polymer (900 μg/mL). The inset shows a 1D spectrum sliced at at 7.4 ppm (red dashed line) from the NOESY spectrum. (B) The measured reduced diffusion coefficient phenytoin (red circle) decreased with increasing polymer concentration in agreement with predictions from a calculated K_b of 44 ± 12 L/mol (red dashed line). The TMSP standard diffusivity (gray diamond) was unaffected.

Next, we selected representative lead systems to scale up for bulk solubilization studies. Spray drying atomizes a volatile liquid stream with heated gas to produce high surface area solid dispersions. Beyond polymer–drug studies, this process recently has been adapted to develop new vaccines[31] and nanobiocomposites.[32] We spray dried phenytoin and nilutamide with representative poly(NIPAm-*co*-DMA) and HPMCAS (as a commercial excipient control) polymers at 10 and 25 wt % drug loading from methanol. We obtained a distribution of micrometer- and nanosized particles, much smaller than pure crystalline drug (Figure S-25). Particle amorphicity was confirmed by powder X-ray diffraction (PXRD) across representative samples at both drug loadings (Figure S-27). The glass transition temperature (T_g) values of the select spray-dried dispersion samples were 80–90 °C (Table S-7), which are expected to provide sufficient solid-state stability based on similar high-T_g excipients.[8,13]

DOI: 10.1021/acscentsci.6b00268
ACS Cent. Sci. 2016, 2, 748–755

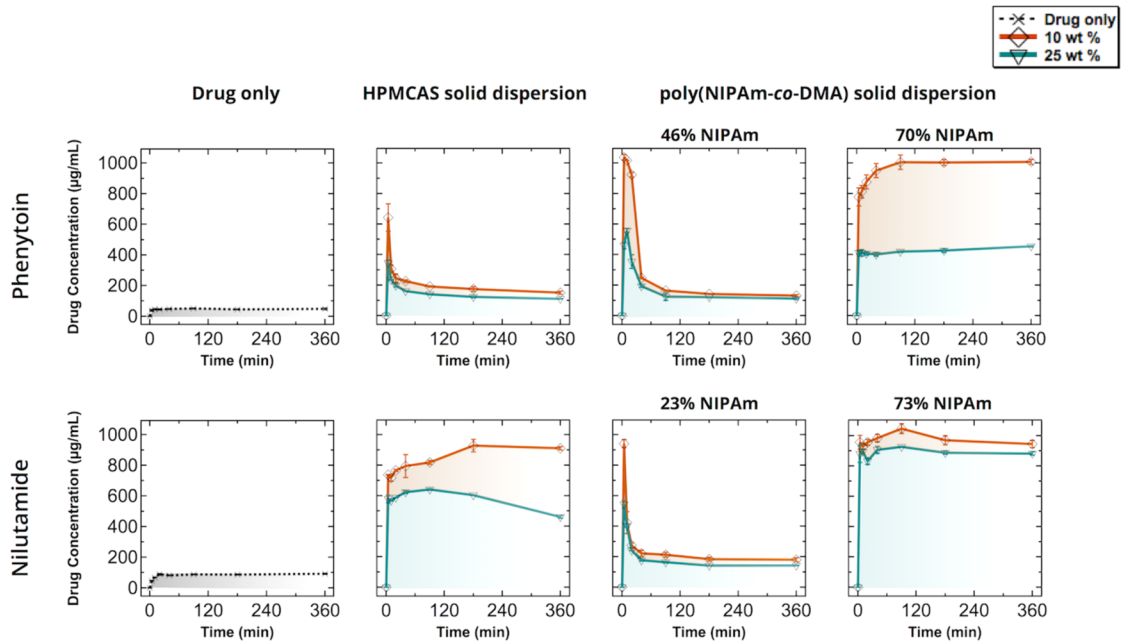

Figure 4. In vitro dissolution tests of representative solid dispersions. Dissolution profiles of phenytoin and nilutamide show supersaturated drug concentration over time for drug only (×, dashed black) and formulations spray dried at 10 wt % (◇, solid dark orange) and 25 wt % (▽, solid dark green). Experiments were prepared with a total drug concentration of 1000 μg/mL. Error bars represent the range of collected data for $N = 2$.

Following conventional nonsink testing protocols,[13] in vitro microcentrifuge dissolution experiments were conducted in PBS at the same SI = 0.09 with 0.5 wt % fasted simulated intestinal fluid powder at 37 °C (Figure 4). We note that the dissolution profiles of the crystalline drug are reported instead of the amorphous drug form due to experimental limitations. Specifically, molten quenching and spray drying phenytoin results in thermal decomposition and incomplete crystallinity suppression in the solid form by PXRD, respectively.[33] Trasi and Taylor have reported the enhanced nucleation propensity of amorphous solid nilutamide at temperatures below the T_g.[34] Thus, we refrain from comparing our results to spray-dried phenytoin and nilutamide in the absence of an excipient. HPMCAS solid dispersions released phenytoin immediately but exhibited rapid desupersaturation to ~200 μg/mL. Ricarte et al. have previously demonstrated that this polymer can store amorphous phenytoin at a length scale of 200 nm using electron energy loss spectroscopy,[35] and thus, the observed precipitation in solution was attributed to an inability to inhibit nucleation and crystal growth. Conversely, HPMCAS was effective in supersaturating nilutamide at 10 wt %; we speculate that its ionized state and amphilicity imparted favorable interactions to nilutamide, akin to other drugs we have previously studied.[18] For the poly(NIPAm-*co*-DMA) systems with both drugs, at low NIPAm incorporations, excipients were more hydrophilic and abandoned drug molecules due to insufficient inhibitor sites. At the 70 mol % NIPAm composition, solid dispersion dissolution achieved full apparent solubilization at 10 wt % and high drug stabilization at 25 wt %. This was equivalent to a 20.8 ± 0.1 and 9.1 ± 0.2 times increase in the area under the dissolution curve (AUC_{360min}) at 360 min, respectively. Continuing to increase the inhibitor content (and thereby reducing polymer hydrophilicity) reduced the drug dissolution performance (Figure S-28). Figure S-30 summarizes the AUC_{360min} enhancement values for all leading and off-composition polymers identified by the high-throughput precipitation inhibition screening. In general, the strong correlation between HTS and in vitro results is promising toward formulating classes of anticonvulsants and antiandrogens, many of which share cyclic imide chemical features.[20]

For in vivo noncompartmental pharmacokinetic (PK) analysis of these solid dispersions with phenytoin, 15 rats were evaluated among five formulation groups (Figure S-31) for 24 h at a 40 mg/kg dose, chosen to satisfy the narrow therapeutic range of the drug.[36] Oral gavage administration of crystalline phenytoin exhibited extremely low PK plasma levels (Figure 5 A). This supports previous reports that its erratic bioavailability is attributed to poor aqueous solubility and incomplete dissolution.[37,38] The HPMCAS system at 10 wt % drug afforded moderate improvement. The average area under the curve (AUC, a metric of oral bioavailability) over 24 h was calculated to be 2360 ± 810 μg/mL-min. To quantify the effectiveness of HPMCAS solid dispersions toward solubilization enhancement, we compared this result to the conventional prodrug strategy of increasing the oral bioavailability for phenytoin.[35] Burstein et al. reported that the AUC over 24 h of fosphenytoin (the approved prodrug of phenytoin) in rat models was 1860 ± 310 μg/mL-min,[38] within the bioavailability performance of HPMCAS solid dispersions. Thus, commercial polymers have the potential to greatly aid the limited solubility of hydrophobic drugs. With solid dispersions, focus on the customization of more specialized excipients for a drug of high therapeutic interest can further elevate this improvement in bioavailability.

For the poly(NIPAm-*co*-DMA) systems, chemical composition and drug loading played clear roles in achieving higher systemic absorption efficacy (Figure 5 B). The AUC at 6 h for the 10 wt % poly(NIPAm70-*co*-DMA30) solid dispersions was statistically different ($p < 0.05$, ANOVA and post hoc analysis) from the 10 wt % HPMCAS and neat phenytoin systems (Figure 5 C), increasing the respective AUC by 3- and 23-fold in improvement. At 24 h, systemic elimination depleted

DOI: 10.1021/acscentsci.6b00268
ACS Cent. Sci. 2016, 2, 748−755

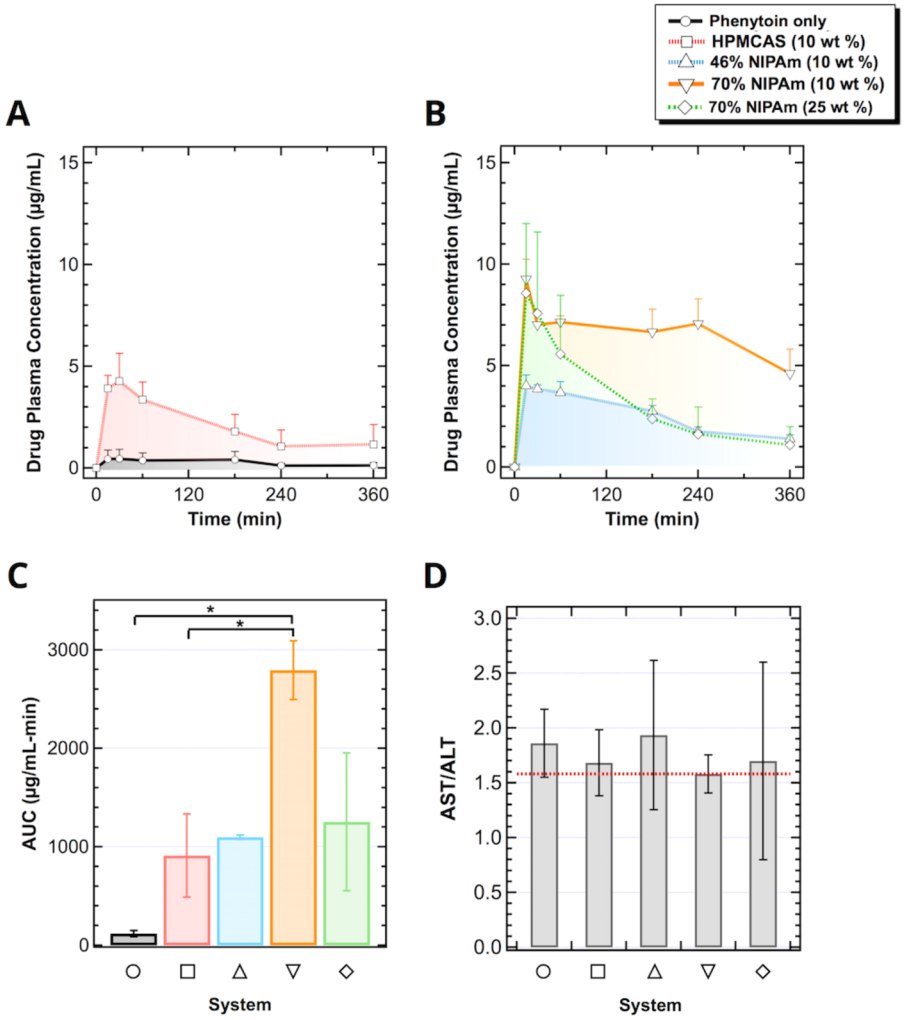

Figure 5. In vivo pharmacokinetics (PK) study of select solid dispersions. PK drug plasma concentration over time is compared between (A) controls phenytoin only (○, solid gray) and HPMCAS spray dried at 10 wt % (□, dashed red) and (B) poly(NIPAm-*co*-DMA) formulations at 46% NIPAm content at 10 wt % (△, dashed blue) and 70% NIPAm content spray dried at 10 (▽, solid orange) and 25 wt % (◇, dashed green). The (C) area under the curve (AUC) and (D) AST/ALT ratio at 6 h provide respective metrics of oral bioavailability and liver toxicity (the dashed red line denotes the AST/ALT of a control animal). All values show the mean + standard error of the mean for $N = 3$. * denotes statistical significance using one-way ANOVA, Welch, and Tukey's HSD tests at $p = 0.05$.

phenytoin plasma levels, but the distinctions remained (Figure S-31). No associated liver toxicity was observed using an AST/ALT assay for all animals (Figure 5 D). Thus, we have demonstrated that the high-throughput excipient discovery process can identify promising polymer candidates for solid dispersion delivery strategies. The fundamental polymer structures and chemical attributes translated to unprecedented in vivo oral bioavailability improvement.

Altogether, the use of high-throughput synthesis and screening for excipients (in tandem with current drug discovery efforts) represents valuable toolsets to probe complex and compositionally dependent properties of a wide class of materials. This rapid polymer discovery process enabled the rational design of pharmaceutical excipients in the form of well-defined synthons for amorphous solid dispersions. A directed library of polymers was studied in a molecular evolution approach to judiciously examine polymer−drug behavior in solution, which is otherwise challenging to predict a priori. These principles can conceivably allow preliminary design rules for robust oral drug delivery structures to be developed in pursuit of better addressing unmet medical needs. Rapid assembly and screening of molecular building blocks paired with revealing characterization techniques can reconcile practical challenges in designing specialized excipients with high precision and specificity, customizing formulation and reformulation efforts of potential blockbuster drugs with new opportunities to lower the needed dose and resultant cost of important medicines for oral drug delivery.

■ ASSOCIATED CONTENT

Supporting Information

The Supporting Information is available free of charge on the ACS Publications website at DOI: 10.1021/acscentsci.6b00268.

Supplemental synthetic procedures, manual and high-throughput RAFT polymerization details, cloud point measurements, precipitation inhibition screening results, 2D NOESY and DOSY NMR experiments, solid dispersion characterization, in vitro dissolution testing results, in vivo PK and AUC statistical analysis, in vivo ALT/AST enzyme toxicity assay, and author roles/responsibilities (PDF)

DOI: 10.1021/acscentsci.6b00268
ACS Cent. Sci. 2016, 2, 748−755

AUTHOR INFORMATION

Corresponding Authors

*E-mail: bates001@umn.edu. Tel: 612-624-0839.
*E-mail: treineke@umn.edu. Tel: 612-624-8042.

Present Address

‡J.M.T.: Institute for Molecular Engineering, University of Chicago, Chicago, Illinois 60637, United States.

Notes

The authors declare no competing financial interest.

ACKNOWLEDGMENTS

The authors gratefully thank Prof. Timothy P. Lodge, Prof. Marc A. Hillmyer, and Dr. Robert L. Schmitt for helpful discussions. We thank Sara M. Ouellette and Linda K. Stoneburner for operating the high-throughput experiments. This work was financially supported by The Dow Chemical Company. J.M.T. acknowledges support from the National Science Foundation (NSF) Graduate Research Fellowship under Grant 00006595 and the University of Minnesota Doctoral Dissertation Fellowship. Part of this work was carried out in the College of Science and Engineering Characterization Facility, University of Minnesota, which has received capital equipment funding from the NSF through the UMN MRSEC program under Award Number DMR-1420013. The University of Minnesota and The Dow Chemical Company have submitted a patent application covering aspects of the work described in this report to the U.S. Patent Office.

REFERENCES

(1) Carino, G. P.; Mathiowitz, E. Oral insulin delivery. *Adv. Drug Delivery Rev.* **1999**, *35*, 249−257.
(2) Prisant, L. M.; Elliott, W. J. Drug delivery systems for treatment of systemic hypertension. *Clin. Pharmacokinet.* **2003**, *42*, 931−940.
(3) Sham, H. L.; Kempf, D. J.; Molla, A.; Marsh, K. C.; Kumar, G. N.; Chen, C. M.; Kati, W.; Stewart, K.; Lal, R.; Hsu, A.; Betebenner, D.; Korneyeva, M.; Vasavanonda, S.; McDonald, E.; Saldivar, A.; Wideburg, N.; Chen, X.; Niu, P.; Park, C.; Jayanti, V.; Grabowski, B.; Granneman, G. R.; Sun, E.; Japour, A. J.; Norbeck, D. W. ABT-378, a highly potent inhibitor of the human immunodeficiency virus protease. *Antimicrob. Agents Chemother.* **1998**, *42*, 3218−3224.
(4) Mitragotri, S.; Burke, P. A.; Langer, R. Overcoming the challenges in administering biopharmaceuticals: formulation and delivery strategies. *Nat. Rev. Drug Discovery* **2014**, *13*, 655−672.
(5) Drews, J. Drug Discovery: A Historical Perspective. *Science* **2000**, *287*, 1960−1964.
(6) Paul, S. M.; Mytelka, D. S.; Dunwiddie, C. T.; Persinger, C. C.; Munos, B. H.; Lindborg, S. R.; Schacht, A. L. How to improve R&D productivity: the pharmaceutical industry's grand challenge. *Nat. Rev. Drug Discovery* **2010**, *9*, 203−214.
(7) Altarum Institute, Center for Sustainable Health Spending data brief: a 10-year projection of the prescription drug share of national health expenditures, including nonretail. October 2014 (accessed Sept 21, 2016).
(8) Williams, H. D.; Trevaskis, N. L.; Charman, S. A.; Shanker, R. M.; Charman, W. N.; Pouton, C. W.; Porter, C. J. H. Strategies to Address Low Drug Solubility in Discovery and Development. *Pharmacol. Rev.* **2013**, *65*, 315−499.
(9) Lipinski, C. A.; Lombardo, F.; Dominy, B. W.; Feeney, P. J. Experimental and computational approaches to estimate solubility and permeability in drug discovery and development settings. *Adv. Drug Delivery Rev.* **2001**, *46*, 3−26.
(10) Roy, D.; Brooks, W. L. A.; Sumerlin, B. S. New directions in thermoresponsive polymers. *Chem. Soc. Rev.* **2013**, *42*, 7214−7243.
(11) Nasongkla, N.; Bey, E.; Ren, J.; Ai, H.; Khemtong, C.; Guthi, J. S.; Chin, S.-F.; Sherry, A. D.; Boothman, D. A.; Gao, J. Multifunctional Polymeric Micelles as Cancer-Targeted, MRI-Ultrasensitive Drug Delivery Systems. *Nano Lett.* **2006**, *6*, 2427−2430.
(12) Ma, X.; Zhao, Y. Biomedical Applications of Supramolecular Systems Based on Host−Guest Interactions. *Chem. Rev.* **2015**, *115*, 7794−7839.
(13) Curatolo, W.; Nightingale, J. A.; Herbig, S. M. Utility of Hydroxypropylmethylcellulose Acetate Succinate (HPMCAS) for Initiation and Maintenance of Drug Supersaturation in the GI Milieu. *Pharm. Res.* **2009**, *26*, 1419−1431.
(14) International Pharmaceutical Excipients Council, http://ipecamericas.org (accessed Sept 21, 2016).
(15) Hancock, B. C.; Parks, M. What is the True Solubility Advantage for Amorphous Pharmaceuticals? *Pharm. Res.* **2000**, *17*, 397−404.
(16) Dalsin, M. C.; Tale, S.; Reineke, T. M. Solution-State Polymer Assemblies Influence BCS Class II Drug Dissolution and Supersaturation Maintenance. *Biomacromolecules* **2014**, *15*, 500−511.
(17) Ting, J. M.; Navale, T. S.; Bates, F. S.; Reineke, T. M. Design of Tunable Multicomponent Polymers as Modular Vehicles To Solubilize Highly Lipophilic Drugs. *Macromolecules* **2014**, *47*, 6554−6565.
(18) Ting, J. M.; Navale, T. S.; Jones, S. D.; Bates, F. S.; Reineke, T. M. Deconstructing HPMCAS: Excipient Design to Tailor Polymer−Drug Interactions for Oral Drug Delivery. *ACS Biomater. Sci. Eng.* **2015**, *1*, 978−990.
(19) Widanapathirana, L.; Tale, S.; Reineke, T. M. Dissolution and Solubility Enhancement of the Highly Lipophilic Drug Phenytoin via Interaction with Poly(N-isopropylacrylamide-*co*-vinylpyrrolidone) Excipients. *Mol. Pharmaceutics* **2015**, *12*, 2537−2543.
(20) World Health Organization, *WHO Model List of Essential Medicines*, 2015 (accessed Sept 21, 2016).
(21) Zipp, G. L.; Rodriguez-Hornedo, N. Growth mechanism and morphology of phenytoin and their relationship with crystallographic structure. *J. Phys. D: Appl. Phys.* **1993**, *26*, B48−B55.
(22) Raynaud, J.-P.; Bonne, C.; Bouton, M.-M.; Lagace, L.; Labrie, F. Action of a non-steroid anti-androgen, RU 23908, in peripheral and central tissues. *J. Steroid Biochem.* **1979**, *11*, 93−99.
(23) Panda, D.; Rathinasamy, K.; Santra, M. K.; Wilson, L. Kinetic suppression of microtubule dynamic instability by griseofulvin: implications for its possible use in the treatment of cancer. *Proc. Natl. Acad. Sci. U. S. A.* **2005**, *102*, 9878−9883.
(24) Buitrago Santanilla, A.; Regalado, E. L.; Pereira, T.; Shevlin, M.; Bateman, K.; Campeau, L. C.; Schneeweis, J.; Berritt, S.; Shi, Z. C.; Nantermet, P.; Liu, Y.; Helmy, R.; Welch, C. J.; Vachal, P.; Davies, I. W.; Cernak, T.; Dreher, S. D. Nanomole-scale high-throughput chemistry for the synthesis of complex molecules. *Science* **2015**, *347*, 49−53.
(25) Li, J.; Ballmer, S. G.; Gillis, E. P.; Fujii, S.; Schmidt, M. J.; Palazzolo, A. M. E.; Lehmann, J. W.; Morehouse, G. F.; Burke, M. D. Synthesis of many different types of organic small molecules using one automated process. *Science* **2015**, *347*, 1221−1226.
(26) Leibfarth, F. A.; Johnson, J. A.; Jamison, T. F. Scalable synthesis of sequence-defined, unimolecular macromolecules by Flow-IEG. *Proc. Natl. Acad. Sci. U. S. A.* **2015**, *112*, 10617−10622.
(27) Guerrero-Sanchez, C.; Keddie, D. J.; Saubern, S.; Chiefari, J. Automated Parallel Freeze−Evacuate−Thaw Degassing Method for Oxygen-Sensitive Reactions: RAFT Polymerization. *ACS Comb. Sci.* **2012**, *14*, 389−394.
(28) Ting, J. M.; Navale, T. S.; Bates, F. S.; Reineke, T. M. Precise compositional control and systematic preparation of multimonomeric statistical copolymers. *ACS Macro Lett.* **2013**, *2*, 770−774.
(29) Sun, D. D.; Ju, T. R.; Lee, P. I. Enhanced kinetic solubility profiles of indomethacin amorphous solid dispersions in poly(2-hydroxyethyl methacrylate) hydrogels. *Eur. J. Pharm. Biopharm.* **2012**, *81*, 149−158.
(30) Lee, J. A.; Lodge, T. P. Polymer-probe Interactions in Forced Rayleih Scattering Measurements of Probe Diffusion in Poly(vinyl acetate) Solutions. *J. Phys. Chem.* **1987**, *91*, 5546−5548.

DOI: 10.1021/acscentsci.6b00268
ACS Cent. Sci. 2016, 2, 748−755

(31) Ohtake, S.; Martin, R. A.; Yee, L.; Chen, D.; Kristensen, D. D.; Lechuga-Ballesteros, D.; Truong-Le, V. Heat-stable measles vaccine produced by spray drying. *Vaccine* **2010**, *28*, 1275−1284.
(32) Johnson, P. E.; Muttil, P.; MacKenzie, D.; Carnes, E. C.; Pelowitz, J.; Mara, N. A.; Mook, W. M.; Jett, S. D.; Dunphy, D. R.; Timmins, G. S.; Brinker, C. J. Spray-Dried Multiscale Nanobiocomposites Containing Living Cells. *ACS Nano* **2015**, *9*, 6961−6977.
(33) Yin, L.; Hillmyer, M. A. Preparation and Performance of Hydroxypropyl Methylcellulose Esters of Substituted Succinates for in Vitro Supersaturation of a Crystalline Hydrophobic Drug. *Mol. Pharmaceutics* **2014**, *11*, 175−185.
(34) Trasi, N. S.; Taylor, L. S. Nucleation and crystal growth of amorphous nilutamide − unusual low temperature behavior. *CrystEngComm* **2014**, *16*, 7186−7195.
(35) Ricarte, R. G.; Lodge, T. P.; Hillmyer, M. A. Nanoscale Concentration Quantification of Pharmaceutical Actives in Amorphous Polymer Matrices by Electron Energy-Loss Spectroscopy. *Langmuir* **2016**, *32*, 7411−7419.
(36) Rundfeldt, C.; Löscher, W. Anticonvulsant efficacy and adverse effects of phenytoin during chronic treatment in amygdala-kindled rats. *J. Pharmacol. Exp. Ther.* **1993**, *266*, 216−223.
(37) Yamaoka, Y.; Roberts, R. D.; Stella, V. J. Low-Melting Phenytoin Prodrugs as Alternative Oral Delivery Modes for Phenytoin: A Model for Other High-Melting Sparingly Water -Soluble Drugs. *J. Pharm. Sci.* **1983**, *72*, 400−405.
(38) Burstein, A. H.; Cox, D. S.; Mistry, B.; Eddington, N. D. Phenytoin pharmacokinetics following oral administration of phenytoin suspension and fosphenytoin solution to rats. *Epilepsy Res.* **1999**, *34*, 129−133.

DOI: 10.1021/acscentsci.6b00268
ACS Cent. Sci. 2016, 2, 748−755